Living Material with Temperature-Dependent Light Absorption

Lealia L. Xiong, Michael A. Garrett, Julia A. Kornfield,* and Mikhail G. Shapiro*

Engineered living materials (ELMs) exhibit desirable characteristics of the living component, including growth and repair, and responsiveness to external stimuli. *Escherichia coli* (*E. coli*) are a promising constituent of ELMs because they are very tractable to genetic engineering, produce heterologous proteins readily, and grow exponentially. However, seasonal variation in ambient temperature presents a challenge in deploying ELMs outside of a laboratory environment because *E. coli* growth rate is impaired both below and above 37 °C. Here, a genetic circuit is developed that controls the expression of a light-absorptive chromophore in response to changes in temperature. It is demonstrated that at temperatures below 36 °C, the engineered *E. coli* increase in pigmentation, causing an increase in sample temperature and growth rate above non-pigmented counterparts in a model planar ELM. On the other hand, at above 36 °C, they decrease in pigmentation, protecting the growth compared to bacteria with temperature-independent high pigmentation. Integrating the temperature-responsive circuit into an ELM has the potential to improve living material performance by optimizing growth and protein production in the face of seasonal temperature changes.

1. Introduction

The field of engineered living materials (ELMs) aims to confer desirable properties of living cells and naturally-occurring biomaterials to designed materials either by incorporating biological cells into a synthetic material, or through the formation of a material by living cells and their synthesized biopolymers.[1–3] These properties include self-assembly, self-healing, and sensing and responding to signals. In the last decade, engineering microbe-derived or living building materials has become of particular interest to researchers because of the possibility of growing these materials in situ, using local resources, obviating the need to transport large amounts of material to remote environments.[4–6] Biomineralized living materials have the potential to comprise the structure of buildings, akin to cement blocks, or to form a protective surface coating, as in roofing shingles or tiles. The cells of microbial species including yeast,[7] cyanobacteria,[4] and *Bacillus subtilis*[8–12] have been used in ELMs, with *Escherichia coli* (*E. coli*) an especially common focus of ELM researchers[2,13–15] because of its extensive characterization and tractability for genetic engineering.[16]

While *E. coli* is a laboratory workhorse, it normally lives in the intestines of warm-blooded animals, where the host maintains a stable temperature of ≈37 °C.[17,18] However, outside of the laboratory or intestinal environment, cells are exposed to fluctuations in temperature, nutrients, and moisture, all of which affect their viability and growth rate. Indeed, *E. coli* is known to live in freshwater and soil only in tropical ecosystems, which maintain an appropriate temperature, nutrient level, and humidity.[17] In the laboratory, the minimum temperature for the growth of *E. coli* is ≈7.5 °C in minimal media,[19] but even a decrease in temperature from 37 °C to 25 °C reduces the rate of growth of *E. coli* cultures in exponential phase by ≈38%.[20] The reduction in growth rate with temperature correlates with a reduced ability to synthesize protein. On the other hand, exposure to temperatures above 37 °C is also detrimental to *E. coli*, with growth inhibited above ≈44 °C, due to protein instability at high temperatures.[21] Thus, exposure to nonideal temperature limits the potential for outdoor environmental or exterior building materials applications for an ELM in which *E. coli* is a living component.

Here, we develop a genetic circuit that senses temperature and turns on the formation of a light-absorptive pigment below 36 °C. We demonstrate that this circuit enables *E. coli* growing in dense patches under simulated sunlight to improve its growth rate over unpigmented *E. coli* at a suboptimal environmental temperature

L. L. Xiong, M. G. Shapiro
Division of Engineering and Applied Sciences
California Institute of Technology
1200 E. California Blvd., Pasadena, CA 91125, USA
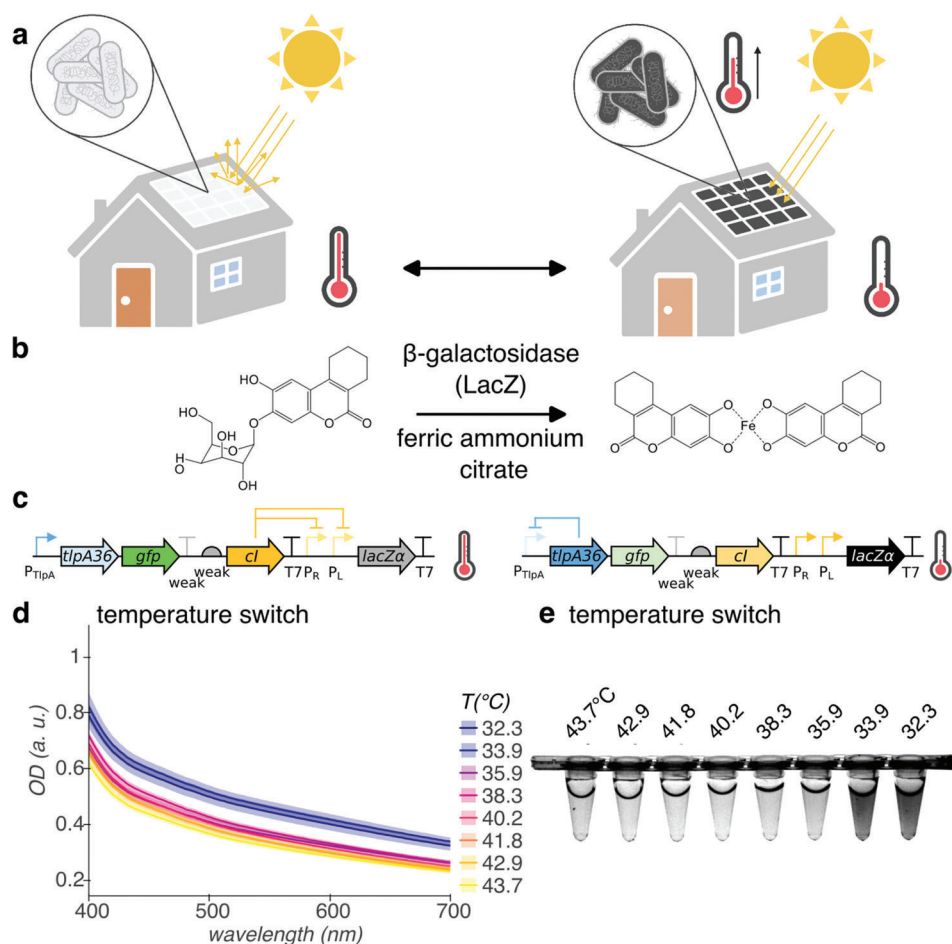E-mail: mikhail@caltech.edu
M. A. Garrett, J. A. Kornfield, M. G. Shapiro
Division of Chemistry and Chemical Engineering
California Institute of Technology
1200 E. California Blvd., Pasadena, CA 91125, USA
E-mail: jak@cheme.caltech.edu
M. G. Shapiro
Howard Hughes Medical Institute
California Institute of Technology
1200 E. California Blvd., Pasadena, CA 91125, USA

Figure 1. Cold-activated production of light-absorptive pigment for *E. coli*-containing ELMs. a) Illustration of ELM used as building material. At ambient temperature greater than or equal to optimum for growth, *E. coli* remains colorless (left). However, at ambient temperatures less than optimal, *E. coli* express light-absorptive pigment, warming under illumination by the sun to recover growth rate (right). Illustration created with BioRender.com. b) Genetically-encodable light-absorptive pigment system. β-galactosidase cleaves S-gal at the glycosidic bond, exposing the esculetin group, which coordinates with ferric iron to form a black pigment. c) Circuit diagram of temperature switch construct for low-temperature pigmentation, with state of regulation arcs, indicated at high and low temperatures. Genes, left to right: *tlpA36*, *gfp*, *cI*, *lacZα*. d,e) Visible light optical density (OD) spectra d) and representative white light transillumination image e) of cultures of *E. coli* containing the temperature switch construct after 24 h growth in pigment-induction media at temperatures ranging from 43.7 °C to 32.3 °C. $n = 4$ biological replicates; shading represents +/− standard error of the mean.

of 32 °C by capturing light and warming up. At the same time, when growing at 42 °C, an above-optimal temperature, our engineered *E. coli* remains unpigmented and grows faster than bacteria with temperature-independent pigmentation. We anticipate that this temperature switch circuit will confer a protective effect on *E. coli* in ELMs on a seasonal basis. During extended periods below 36 °C, the cells will produce pigment and improve growth throughout the cool season. However, they will stop producing pigment for the hot season, when light absorption becomes detrimental.

2. Results

E. coli within ELMs in outdoor applications, such as building exteriors, will be exposed to changes in ambient temperature, which will challenge their ability to grow and produce proteins of interest. For *E. coli*, the optimal growth temperature is 37 °C. We

propose that when the ambient temperature drops below the optimum, the cells should produce a light-absorptive pigment, allowing them to warm up when exposed to sunlight, whereas at or above the optimum, they should remain unpigmented, to avoid overheating (**Figure 1**a).

We repurposed a chemical compound designed to enable the use of β-galactosidase as a gene reporter, 3,4-cyclohexenoesculetin-β-D-galactopyranoside (S-gal), as our genetically-encodable pigment (Figure 1b). S-gal, which is yellow in solution, consists of galactose linked to 3,4-cyclohexenoesculetin by a glycosidic bond. β-galactosidase hydrolyzes this bond, which frees the esculetin group to complex with ferric iron (provided in the growth medium as ferric ammonium citrate, which is brown in solution) to form a black light-absorptive pigment.[22]

We used the TlpA36 transcriptional repressor as a genetically-encodable sensor with a temperature threshold of 36 °C[23]

and constructed a gene circuit to invert its action, enabling *E. coli* to turn on enzymatic pigment production below 36 °C (Figure 1c). At these temperatures, TlpA36 represses expression of CI repressor from the P_{TlpA} promoter. The LacZα peptide of β-galactosidase, which presents a much lower metabolic burden to the cell than the complete enzyme, is expressed from the CI-regulated P_R-P_L tandem promoter. Above 36 °C, TlpA36 loses repressor function, so CI repressor is expressed from the P_{TlpA} promoter and represses expression of LacZα. The concentration of CI repressor is tuned down by placing a weak terminator and weak ribosome binding site upstream. The complementary LacZω peptide is induced from the genome of *E. coli* DH10B by addition of isopropyl β-D-1-thiogalactopyranoside (IPTG) to the growth medium; neither LacZα nor LacZω are enzymatically active on their own, but combine to form functional β-galactosidase.[24] mWasabi (GFP) serves as a marker of high temperature.

We measured the optical density (OD) at visible light wavelengths of planktonic *E. coli* DH10B containing our temperature switch construct after growth in pigment induction media (containing S-gal, ferric ammonium citrate, and IPTG) at temperatures ranging from 43.7 °C to 32.3 °C (Figure 1d,e; Figure S3, Supporting Information). Cultures of *E. coli* containing the temperature switch construct increase in optical density across the visible light spectrum from 400 – 700 nm below 35.9 °C, compared to at and above 35.9 °C. In comparison, cultures of *E. coli* containing a pigmented control construct (Tables S1 and S2 and Figure S1, Supporting Information) exhibit high optical density across the visible light spectrum from 32.3 °C through 42.9 °C, with a decrease at the highest temperature of 43.7 °C (Figures S2 and S3, Supporting Information). These measurements include both the absorbance of light by the pigment (if present) and the scattering of light due to the presence of cells, as both would contribute to heat transfer with illumination. The OD600 of cultures of *E. coli* grown at temperatures in this range is maximal at 37–38 °C (Figure S4, Supporting Information). Extracellular pigment in filtered media shows higher optical density across the visible light spectrum than filtered media containing S-gal and ferric ammonium citrate (Figure S5, Supporting Information).

After constructing the temperature switch for expression of pigment below 36 °C and demonstrating its function in liquid culture, we grew *E. coli* containing the construct in a dense, centimeter-scale patch format to simulate the environment of an ELM. We suction-coated a suspension of cells grown to saturation overnight at 38 °C onto a polycarbonate membrane backing and placed it on a media-saturated melamine foam growth substrate (**Figure 2**a). We placed the samples in a home-built illuminated growth chamber and monitored the relative temperature of the samples compared to the melamine foam using a lightweight 32 × 24 thermal IR sensor array (Figure 2b). The LED light source was placed at a distance of 120 mm from the samples to achieve an average light flux of 120 000 lx, slightly higher than direct sunlight. Between the light source and the samples, we placed a 3.175 mm sheet of glass to filter IR and a 1.5 mm sheet of colorless, transparent acrylic to filter UV, while allowing visible light illumination of the samples. We placed the thermal IR sensor array on a motorized arm that retracts when not imaging to avoid casting a shadow. After 48 h growth in illuminated conditions at 42 °C, patches of *E. coli* containing our tempera-ture switch construct produce little pigment, whereas, at 32 °C, they become nearly opaque when imaged with white light transillumination (Figure 2c; Figure S10, Supporting Information). Because the melamine foam is opaque in transillumination, we transferred the patches of *E. coli* on their polycarbonate membranes to LB agar plates for imaging.

We tested the ability to turn on pigmentation to confer protection against slowed growth at 32 °C with and without illumination by comparing the growth rate of *E. coli* containing our temperature switch construct against the growth rate of *E. coli* containing a control construct encoding mWasabi under the control of TlpA36[23] (unpigmented control). While patches containing our temperature switch construct express pigment at this temperature, the control patches have no mechanism for pigment production and remain translucent (**Figure 3**a; Figures S8 and S9, Supporting Information). Due to the low spatial resolution of the sensor array, the precise temperature of the samples cannot be determined; however, the pigmented patches clearly warm above the background temperature (Figure 3b).

We monitored the growth of the patches via their thickness, quantified from optical coherence tomography cross-sectional images, and their area, quantified from white light transillumination images. With illumination, the patches containing the temperature switch construct grow to twice the thickness of patches containing the control construct over the course of 72 h (Figure 3c–e; Figure S6a,b, Supporting Information), whereas without illumination, the patches grow to the same thickness at each timepoint (Figure 3f; Figure S6c,d, Supporting Information). In addition, with illumination, the temperature switch allows the patches to grow in area linearly with time, while the rate of increase in area of unpigmented patches slows over time (Figure 3g, Figure S7a, Supporting Information). On the other hand, without illumination, patches containing both constructs grow in area linearly at approximately the same rate (Figure 3h; Figure S7b, Supporting Information). Due to lower humidity in the home-built illuminated growth chamber than in the incubator used for growth without illumination, the amount of growth with and without illumination cannot be directly compared. However, our results suggest that expressing pigment at 32 °C using the temperature switch construct gives *E. coli* in a dense patch format a growth advantage under illumination compared with unpigmented patches.

While pigmentation is advantageous at below-optimal ambient temperatures, we hypothesized that it would be deleterious at above-optimal temperatures by exacerbating overheating. To test this hypothesis, we compared the growth at 42 °C of patches of *E. coli* containing our temperature switch construct against the growth rate of *E. coli* containing a control construct encoding IPTG-inducible LacZα (pigmented control). We supplemented the media with 0.1% D-glucose to catabolically repress[25] the expression of LacZω (and hence, the formation of pigment) during sample preparation at room temperature and while the samples equilibrated to 42 °C. After 48 h, the patches containing our temperature switch construct lack pigmentation and appear translucent, while the control patches turn black and opaque, warming above the background temperature (**Figure 4**a,b).

To avoid exposing the samples to laboratory room temperatures of 16 – 25 °C by handling them during the experiment,

2301730 (3 of 8)
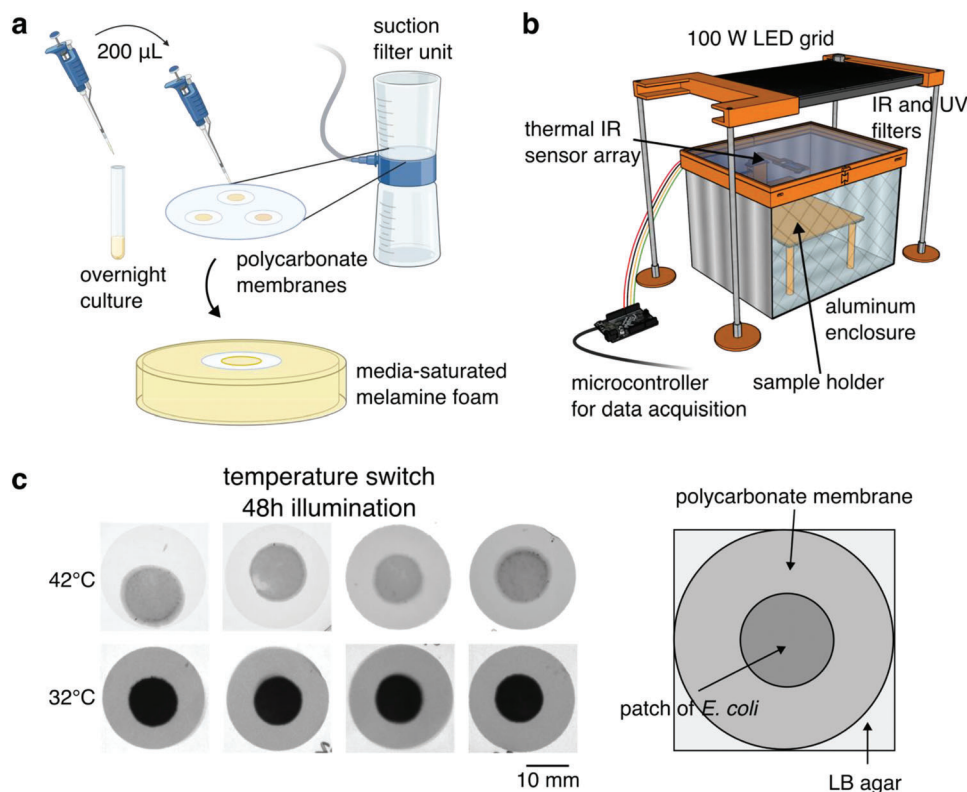
Figure 2. Temperature-dependent pigmentation in a model ELM. a) Schematic of formation of dense, centimeter-scale patches of *E. coli* to simulate the ELM environment. We grew *E. coli* overnight to saturation in a liquid medium. For each patch, we transferred 200 μL of culture to track-etched polycarbonate membranes (25 mm diam., 0.2 μm pores) and applied suction to coat the cells onto the membranes, forming a dense patch. We then transferred the coated membranes to a melamine foam substrate saturated with liquid media for growth. b) Schematic of illuminated growth chamber. We used a 100 W white light LED to expose *E. coli* patches to illumination and monitored the temperature using a 32×24 array of thermal IR sensors. The sensor array is attached to a motorized arm and retracts when not imaging to avoid shadowing the samples. c) Transillumination white light images of patches of *E. coli* containing the temperature switch construct on polycarbonate membranes after 48 h growth in the illuminated growth chamber with pigment-induction media at 42 °C and 32 °C. Parts of figure created with BioRender.com.

we measured the area and thickness of the patches only at the endpoint of 48 h. The area of the patches containing the temperature switch compared with the patches containing the pigmented control showed no statistical difference either with or without illumination (Figure S12, Supporting Information). However, the patches containing the temperature switch were thicker than the patches containing the control construct under illumination (Figure 4c–e, Figure S11a, Supporting Information). Without illumination, the patch thickness was not statistically different ($p = 0.1214$), although there was a trend toward greater thickness for the switch, potentially due to the burden of protein overexpression from the IPTG-induced control construct (Figure 4f, Figure S11b, Supporting Information). Thus, turning off expression of pigment at 42 °C using the temperature switch construct confers an advantage on *E. coli* in a dense patch format grown under illumination compared with temperature-independent, chemically-induced pigmentation.

3. Discussion

This work establishes a proof of concept for a genetically-encoded mechanism for supporting *E. coli* in an ELM under non-optimal ambient temperature. We demonstrated a genetic circuit for ex-

pression of a dark, light-absorptive pigment below 36 °C. At 32 °C, dense patches of *E. coli* containing this circuit become nearly opaque with black pigment, allowing them to warm above background and grow in both area and thickness at a greater rate than unpigmented patches. Conversely, at 42 °C, patches remain translucent, avoiding further overheating and growing to a greater thickness than chemically-induced pigmented patches. Because *E.coli*-based ELMs rely on *E. coli* growth and protein production to form the material, as well as confer engineered properties, such as environmental sensing, to the material, long-term exposure to temperatures below or above 37 °C will be detrimental to their function. Our temperature switch genetic construct is in principle compatible with any cloning strain of *E. coli* with the *lacZΔM15* genotype, allowing it to be used in existing *E. coli*-based ELMs, such as biomineralized *E. coli* biofilms.[26,27]

While this study provides a proof of concept for temperature self-regulation, additional work is needed to improve the kinetics of the temperature switch. Because our system does not include a mechanism for degradation of the pigment complex, even brief low-temperature excursions allow pigment to accumulate in the ELM. While protective in the case of long-term exposure to low temperatures, this could cause overheating once the ambient temperature reaches 37 °C or above.
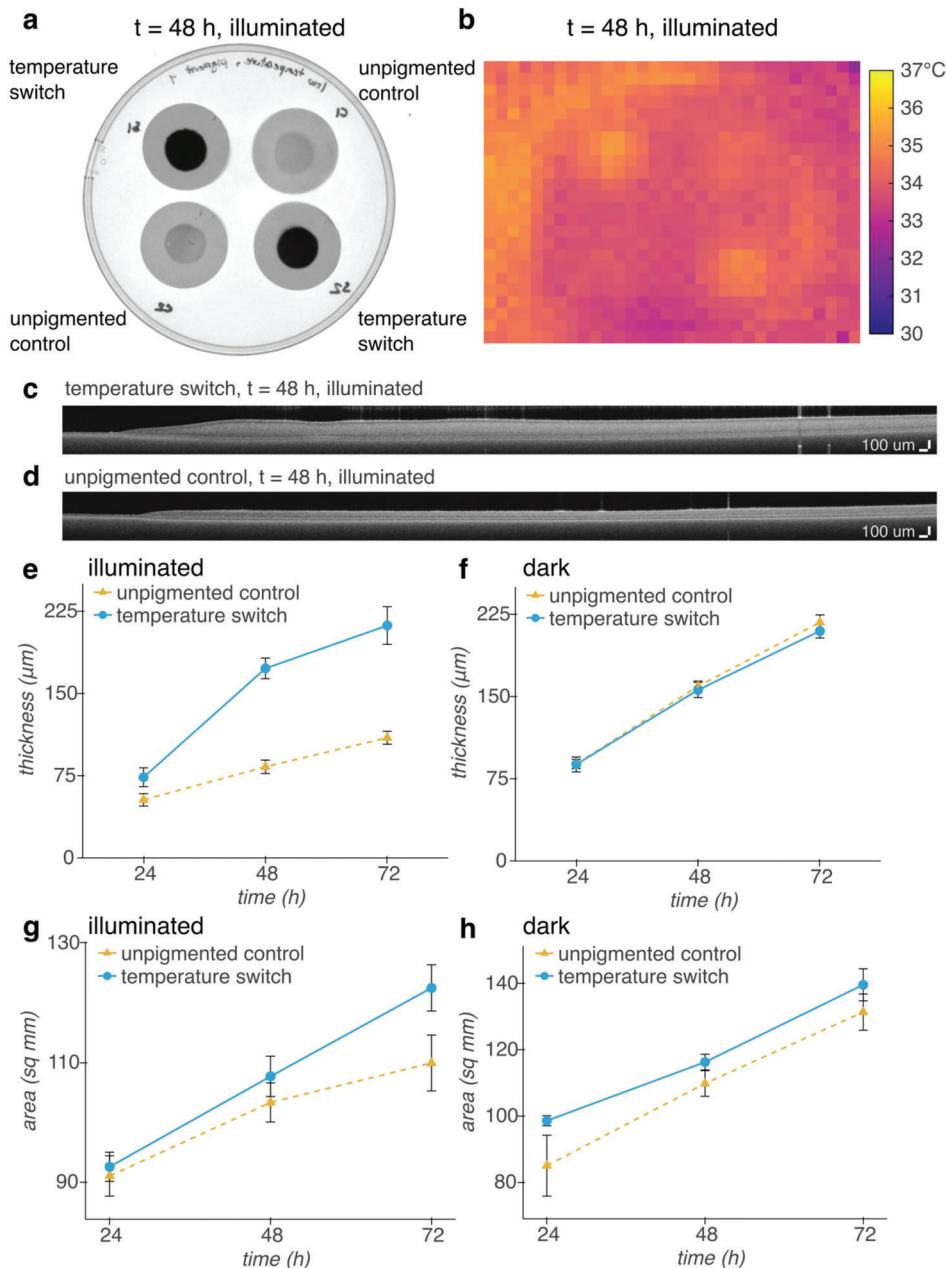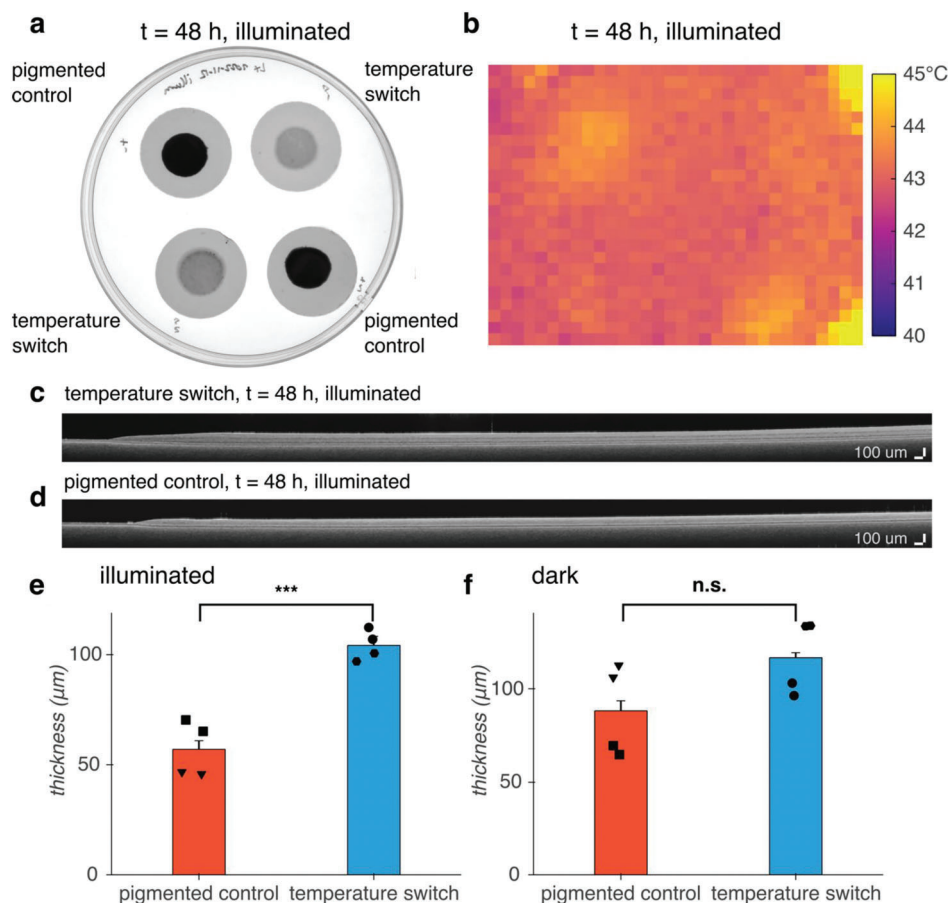
Figure 3. Cold-induced pigment improves the growth of dense patches of *E. coli* under illumination at 32 °C. a) White light transillumination image of patches of *E. coli* containing either our temperature switch construct or an unpigmented control construct encoding heat-inducible GFP after transferring to agar for imaging at 48 h. b) Thermal IR image of patches inside illuminated growth chamber at 48 h. c,d) Representative OCT images of patches of *E. coli* containing our temperature c) switch construct, or d) the unpigmented control construct. e,f) Thickness of patches grown e) under illumination, or f) in a dark incubator over time. The slower rate of evaporation without illumination allows for thicker growth overall than with illumination. g,h) Area of patches grown g) under illumination or h) in a dark incubator over time. *n* = 4 biological replicates; error bars represent +/− standard error of the mean.

To avoid producing pigment at night in climates or seasons where day-time temperatures exceed 37 °C, but night-time temperatures drop below, our circuit could be modified to incorporate a light sensor, such as phytochrome,[30] using an AND gate,[31] turning on pigment production only with both light and cold temperature. In addition, to accelerate the transition from dark to translucent in response to a change in environment from low to high temperature, an enzyme cassette for biodegradation of the esculetin-based pigment could be developed from coumarin degradation pathways found in soil bacteria.[32] To increase protection from heat, this degradation cassette, or a cassette encoding light-scattering proteins such as gas vesicles,[33,34] could be turned on at high temperature in place of the GFP marker currently incorporated in our construct, clearing pigment from the ELM or scattering incoming light.

Finally, the S-gal-derived black pigment used in our system is deposited extracellularly (Figure S13, Supporting Information). Additionally, a possible alternative light-absorptive pigment, eu-

**ADVANCED
SCIENCE NEWS**

www.advancedsciencenews.com

**ADVANCED
SCIENCE**
Open Access

www.advancedscience.com

Figure 4. Turning off pigmentation above 36 °C improves the growth of dense patches of *E. coli* under illumination at 42 °C compared to a pigmented control. a) White light transillumination image of patches of *E. coli* containing either the temperature switch construct or a pigmented control construct encoding IPTG-inducible LacZα after transferring to agar for imaging at 48 h. b) Thermal IR image of patches inside illuminated growth chamber at 48 h. c,d) Representative OCT images of patches of *E. coli* containing our c) temperature switch construct or d) the pigmented control construct. e,f) Thickness of patches grown e) under illumination ($p = 0.0006$) or f) in a dark incubator ($p = 0.1214$) at 48 h. Inverted triangle and hexagon markers indicate patches coated onto Whatman Nucleopore polycarbonate membranes; square and circle markers indicate patches coated onto Sartorius polycarbonate membranes. $n = 4$ biological replicates; error bars represent +/− standard error of the mean. p-values calculated using a two-tailed unpaired t-test; *** $p \leq 0.001$, n.s. $p \geq 0.05$.

melanin, can be produced extracellularly by *E. coli* via expression of tyrosinase.[35,36] Tyrosinase oxidizes tyrosine intracellularly, but polymerization of eumelanin is completed outside the cell. For both S-gal-derived pigment and eumelanin, pigment degradation enzymes thus need to be exported outside the cell to remove the pigment. However, it may be possible for future mechanisms for ELM media exchange – bringing fresh nutrients to the ELM and removing waste – to also wash away pigment. In this scenario, the pigment would be replaced only when it is needed, during periods of cool temperature. With our thermal bioswitch circuits and these future improvements, ELMs will gain the ability to harness sunlight to keep warm or stay cool in the face of seasonal temperature changes.

4. Experimental Section

Plasmid Construction and Molecular Biology: All plasmids were designed using SnapGene (GSL Biotech) and assembled via reagents from New England Biolabs for KLD mutagenesis (E0554S) or HiFi Assembly (E2621L). After assembly, constructs were transformed into NEB Turbo (C2984I) *E. coli* for growth and plasmid preparation. Integrated DNA Technologies synthesized all PCR primers. TlpA36 and mWasabi[37] (GFP) were obtained from our previous work.[23] LacZα was tagged at the C-terminus with the AAV ssrA tag[38] (amino acid sequence AAN-DENYAAAV). The weak terminator in the temperature switch construct is Part:BBa_B1002.[39] The weak RBS in the temperature switch construct is RBSF.[40] Plasmids were transformed into DH10B *E. coli* (ThermoFisher) for downstream experiments. Gene circuit diagrams were created using the DNAplotlib[41] library in Python.

Visible Light Absorbance Assays: 1 mL cultures of LB medium (Sigma) with 100 µg mL^{-1} ampicillin were inoculated with a single colony per culture and grown at 38 °C, 250 rpm for 18.5 h. 30 µL were diluted into 2 mL LB with 300 µg mL^{-1} 3,4-cyclohexenoesculetin-β-D-galactopyranoside (S-gal) (Sigma), 500 µg mL^{-1} ferric ammonium citrate (Sigma), 100 µM IPTG, 100 µg mL^{-1} ampicillin and propagated at 38 °C, 250 rpm for 90 min. The cultures were dispensed in 100 µL aliquots into 8-well PCR strips (Bio-Rad) and incubated for 24 h in a thermal gradient using a DNA Engine Tetrad 2 Peltier Thermal Cycler (Bio-Rad) with the lid set to 50 °C. PCR strips were imaged using a ChemiDoc MP Gel Imaging System (Bio-Rad). Contrast

was adjusted using ImageJ software.[42] 90 μL were transferred into 96-well plates (Corning 3631) and absorbance spectra were measured using a Spark multi-mode microplate reader (Tecan). Data analysis was performed using custom Python scripts.

Preparation of Dense Patches of E. coli: Cultures of LB medium (2 mL) (Sigma) with 100 μg mL^{-1} ampicillin (and 25 μM IPTG for pigmented controls) were inoculated with a single colony per culture and grown at 38 °C, 250 rpm for 18.5 h. Nalgene Rapid-Flow sterile disposable filter units (cellulose nitrate, 75 mm diameter, 0.2 μm pore size) (ThermoFisher 450-0020) were rinsed with 1x PBS (Corning) and track-etched polycarbonate membranes (25 mm diameter, 0.2 μm pore size) (Sartorius 23007 unless Whatman Nuclepore 10417006 is indicated) were placed on the filter surface. 200 μL bacterial culture was dispensed onto each membrane and a vacuum was applied to the filter unit to coat the cells onto the membrane. *E. coli* containing the temperature switch construct and the unpigmented control construct express mWasabi after the overnight growth at 38 °C, so the freshly prepared membranes were imaged in epifluorescence using a ChemiDoc MP Gel Imaging System (Bio-Rad) to confirm that the *E. coli* were coated onto the membranes. The thickness of the freshly prepared patches was below the axial resolution of the optical coherence tomography system and the freshly prepared patches were undetectable using transillumination white light imaging.

Growth of E. coli Patches in ELM-like Conditions: LB medium (90 mL (32 °C experiments) or 100 mL (42 °C experiments)) (Sigma) with 75 μg mL^{-1} S-gal, 125 μg mL^{-1} ferric ammonium citrate, 25 μM IPTG, 100 μg mL^{-1} ampicillin (and 0.1% D-glucose for 42 °C experiments) was added to ≈0.7 g melamine foam (Amazon) in a petri dish until foam was saturated. For 42 °C experiments, the saturated foam was prewarmed using a heat lamp. Patches of *E. coli* coated on polycarbonate membranes were placed onto the surface of the saturated foam. Patches were incubated either in a custom illuminated incubator or in a conventional incubator for 72 h (32 °C experiments) or 48 h (42 °C experiments). At 24 h intervals, Petri dishes were weighed to determine the amount of evaporation and the equivalent volume of LB with 75 μg mL^{-1} S-gal, 125 μg mL^{-1} ferric ammonium citrate, 25 μM IPTG, 100 μg mL^{-1} ampicillin (and 0.1% D-glucose for 42°C experiments) at room temperature (for 32 °C experiments) or prewarmed to 42 °C (for 42 °C experiments) was added.

Design and Construction of Illuminated Incubator with In Situ Temperature Monitoring: The enclosure of the illuminated incubator was a 203.2 mm × 254 mm × 180.34 mm aluminum box with a lid consisting of a 3.175 mm layer of glass (IR-filtering) and a 1.5 mm layer of acrylic (UV-filtering) held in a 3D-printed polylactic acid (PLA) collar. The weatherproofing foam was used to provide a tight fit between the lid and the box. The sample holder was located 120 mm from the 100 W LED grid light source (Mifxion), receiving an average light flux of 120 000 lx. The light source was plugged into a power relay (Digital Loggers). The light source heats the interior of the chamber; the temperature was adjusted by adding or removing insulation.

An MLX90640 32 × 24 thermal IR sensor array (Grove or Adafruit) was attached to an SG92R micro servo motor (Tower Pro) via 3D-printed PLA fittings reinforced with wooden craft sticks for monitoring the samples. MCP9808 temperature sensors (Adafruit) were used to monitor the air temperature inside and outside the sample enclosure. All sensors, the servo motor, and the power relay were connected to a Feather M4 Express microcontroller (Adafruit) for data acquisition and control. A custom Bokeh application was used to interface with the microcontroller.

For comparison, *E. coli* patches were grown without illumination using a conventional incubator, as turning off the light source or shading the samples in the illuminated growth chamber would result in lowering the ambient temperature.

Imaging and Analysis of E. coli Patches: *E. coli* patches on polycarbonate membranes were transferred from melamine foam growth substrate to 20 mL PBS agar plates for imaging.

White light transillumination imaging was performed using a ChemiDoc MP Gel Imaging System (Bio-Rad). *E. coli* patch area was measured by using the Canny edge detector algorithm for image segmentation to find the edges of each patch, counting the number of pixels within each patch, and converting to area in square millimeters. In addition, pixel intensity

was quantified (normalized to polycarbonate membrane background and opaque black plastic) and averaged. Analysis was performed via custom Python scripts.

Optical coherence tomography was performed using a Ganymede 210 Series Spectral Domain OCT Imaging System with an OCTP-900 scanner and 8 μm lateral resolution scan lens (Thorlabs). Cross-sectional images with a 10 mm / 2560 pixel (*x*) by 1 mm / 491 pixels (*z*) field of view were acquired at a 5.5 kHz A-scan rate with 7 B-scan averages and 5 A-scan averages per acquisition. The despeckle filter in the ThorImageOCT software (Thorlabs) was applied before exporting. *E. coli* patch thickness was measured using a custom Python script. Briefly, after applying a Gaussian filter, the three narrowest peaks with height and width fulfilling adjustable thresholds were detected in each column and arranged by distance from the top of the image to correspond with the top of the patch, the top of the polycarbonate membrane, and the bottom of the polycarbonate membrane. The vectors for each interface were Hampel filtered to reduce outliers due to imaging artifacts. The thickness was defined as the distance from the top of the patch to the top of the polycarbonate membrane. The mean thickness and standard deviation of each patch between $x = 3.5$ mm and $x = 9.0$ mm (avoiding the edges of the patch) were calculated. Then, the mean for each construct, illumination condition, and temperature was calculated, propagating the standard deviation to calculate the standard error of the mean.

Statistical Analysis: Continuous variables were expressed as mean +/- standard error of the mean. The sample size was $n = 4$ biological replicates. Plasmid for each genetic circuit construct was transformed into *E. coli* and colonies were cultured on agar plates; each biological replicate was a bacterial culture derived from a single colony. Groups (e.g., pigmented control samples versus temperature switch samples) were compared using a two-tailed unpaired *t*-test. Statistical significance was defined as $p \leq 0.05$. Statistical analysis was performed using the Python SciPy Stats package.

Supporting Information

Supporting Information is available from the Wiley Online Library or from the author.

Acknowledgements

Conflict of Interest

The authors declare no conflict of interest.

Author Contributions

L.L.X. and M.G.S. conceived the study. L.L.X. and M.A.G. planned and performed experiments. L.L.X. analyzed data. J.A.K. provided input on research design and data interpretation. L.L.X. and M.G.S. wrote the manuscript with input from all other authors. M.G.S. and J.A.K. supervised the research.

Data Availability Statement

The data that support the findings of this study are available from the corresponding author upon reasonable request.

Keywords

[1] P. Q. Nguyen, N.-M. D. Courchesne, A. Duraj-Thatte, P. Praveschotinunt, N. S. Joshi, *Adv. Mater.* **2018**, *30*, 1704847.
[2] C. Gilbert, T. Ellis, *ACS Synth. Biol.* **2019**, *8*, 1.
[3] S. Liu, W. Xu, *Front. Sens.* **2020**, 1.
[4] C. M. Heveran, S. L. Williams, J. Qiu, J. Artier, M. H. Hubler, S. M. Cook, J. C. Cameron, W. V. Srubar, *Matter* **2020**, *2*, 481.
[5] L. J. Rothschild, *Biochem. Soc. Trans.* **2016**, *44*, 1158.
[6] C. Verseux, M. Baqué, K. Lehto, J.-P. P. de Vera, L. J. Rothschild, D. Billi, *Int J Astrobiol* **2016**, *15*, 65.
[7] L. K. Rivera-Tarazona, T. Shukla, K. A. Singh, A. K. Gaharwar, Z. T. Campbell, T. H. Ware, *Adv. Funct. Mater.* **2022**, *32*, 2106843.
[8] J. Huang, S. Liu, C. Zhang, X. Wang, J. Pu, F. Ba, S. Xue, H. Ye, T. Zhao, K. Li, Y. Wang, J. Zhang, L. Wang, C. Fan, T. K. Lu, C. Zhong, *Nat. Chem. Biol.* **2019**, *15*, 34.
[9] L. M. González, N. Mukhitov, C. A. Voigt, *Nat. Chem. Biol.* **2020**, *16*, 126.
[10] S.-Y. Kang, A. Pokhrel, S. Bratsch, J. J. Benson, S.-O. Seo, M. B. Quin, A. Aksan, C. Schmidt-Dannert, *Nat. Commun.* **2021**, *12*, 7133.
[11] S. Sim, Y. Hui, D. A. Tirrell, *Biomacromolecules* **2022**, *23*, 4687.
[12] H. Jo, S. Sim, *ACS Appl. Mater. Interfaces* **2022**, *14*, 20729.
[13] K. C. Heyde, F. Y. Scott, S.-H. Paek, R. Zhang, W. C. Ruder, *JoVE J. Vis. Exp.* **2017**, *121*, e55300.
[14] A. M. Duraj-Thatte, N.-M. D. Courchesne, P. Praveschotinunt, J. Rutledge, Y. Lee, J. M. Karp, N. S. Joshi, *Adv. Mater.* **2019**, *31*, 1901826.
[15] S. Guo, E. Dubuc, Y. Rave, M. Verhagen, S. A. E. Twisk, T. van der Hek, G. J. M. Oerlemans, M. C. M. van den Oetelaar, L. S. van Hazendonk, M. Brüls, B. V. Eijkens, P. L. Joostens, S. R. Keij, W. Xing, M. Nijs, J. Stalpers, M. Sharma, M. Gerth, R. J. E. A. Boonen, K. Verduin, M. Merkx, I. K. Voets, T. F. A. de Greef, *ACS Synth. Biol.* **2020**, *9*, 475.
[16] Z. D. Blount, *eLife* **2015**, *4*, 05826.
[17] M. D. Winfield, E. A. Groisman, *Appl. Environ. Microbiol.* **2003**, *69*, 3687.
[18] J. D. van Elsas, A. V. Semenov, R. Costa, J. T. Trevors, *ISME J* **2011**, *5*, 173.
[19] M. K. Shaw, A. G. Marr, J. L. Ingraham, *J. Bacteriol.* **1971**, *105*, 683.
[20] R. J. Broeze, C. J. Solomon, D. H. Pope, *J. Bacteriol.* **1978**, *134*, 861.
[21] B. Rudolph, K. M. Gebendorfer, J. Buchner, J. Winter, *J. Biol. Chem.* **2010**, *285*, 19029.
[22] C. A. Voigt, *Synthetic Biology: Methods for Part/Device Characterization and Chassis Engineering*, Academic Press, Cambridge, MA, USA **2011**.
[23] D. I. Piraner, M. H. Abedi, B. A. Moser, A. Lee-Gosselin, M. G. Shapiro, *Nat. Chem. Biol.* **2017**, *13*, 75.
[24] A. Ullmann, D. Perrin, F. Jacob, J. Monod, *J. Mol. Biol.* **1965**, *12*, 918.
[25] B. Magasanik, *Cold Spring Harb. Symp. Quant. Biol.* **1961**, *26*, 249.
[26] Y. Wang, B. An, B. Xue, J. Pu, X. Zhang, Y. Huang, Y. Yu, Y. Cao, C. Zhong, *Nat. Chem. Biol.* **2021**, *17*, 351.
[27] L. Zorzetto, E. Scoppola, E. Raguin, K. G. Blank, P. Fratzl, C. M. Bidan, *Chem. Mater.* **2023**, *35*, 2762.
[28] M. A. Gitt, L. F. Wang, R. H. Doi, *J. Biol. Chem.* **1985**, *260*, 7178.
[29] R. Breitling, A. V. Sorokin, D. Behnke, *Gene* **1990**, *93*, 35.
[30] A. Levskaya, A. A. Chevalier, J. J. Tabor, Z. B. Simpson, L. A. Lavery, M. Levy, E. A. Davidson, A. Scouras, A. D. Ellington, E. M. Marcotte, C. A. Voigt, *Nature* **2005**, *438*, 441.
[31] J. C. Anderson, C. A. Voigt, A. P. Arkin, *Mol Syst Biol* **2007**, *3*, 133.
[32] A. Krikštaponis, R. Meškys, *Mol. J. Synth. Chem. Nat. Prod. Chem.* **2018**, *23*, 2613.
[33] A. E. Walsby, *Microbiol Rev* **1994**, *58*, 94.
[34] R. W. Bourdeau, A. Lee-Gosselin, A. Lakshmanan, A. Farhadi, S. R. Kumar, S. P. Nety, M. G. Shapiro, *Nature* **2018**, *553*, 86.
[35] G. della-Cioppa, S. J. Garger, G. G. Sverlow, T. H. Turpen, L. K. Grill, *Bio/Technology* **1990**, *8*, 634.
[36] V. H. Lagunas-Muñoz, N. Cabrera-Valladares, F. Bolívar, G. Gosset, A. Martínez, *J. Appl. Microbiol.* **2006**, *101*, 1002.
[37] H. Ai, S. G. Olenych, P. Wong, M. W. Davidson, R. E. Campbell, *BMC Biol.* **2008**, *6*, 13.
[38] "Part:BBa_I11012," can be found under, http://parts.igem.org/Part: BBa_I11012, **n.d**.
[39] "Part:BBa_B1002," can be found under, http://parts.igem.org/Part: BBa_B1002, **n.d**.
[40] A. Levin-Karp, U. Barenholz, T. Bareia, M. Dayagi, L. Zelcbuch, N. Antonovsky, E. Noor, R. Milo, *ACS Synth. Biol.* **2013**, *2*, 327.
[41] B. S. Der, E. Glassey, B. A. Bartley, C. Enghuus, D. B. Goodman, D. B. Gordon, C. A. Voigt, T. E. Gorochowski, *ACS Synth. Biol.* **2017**, *6*, 1115.
[42] C. A. Schneider, W. S. Rasband, K. W. Eliceiri, *Nat. Methods* **2012**, *9*, 671.